

WINDOW CONTRIBUTIONS TO a_μ & THE LATTICE-DISPERSIVE HVP DISCREPANCY

Kim Maltman, York University

with Genessa Benton, Diogo Boito, Maarten Golterman, Alex Keshavarzi and Santi Peris



DB, MG, KM, SP, PRD105 (2022) 093003 [2203.05070 [hep-ph]]

DB, MG, KM, SP, PRD107 (2023) 034512 [2210.13677 [hep-ph]]

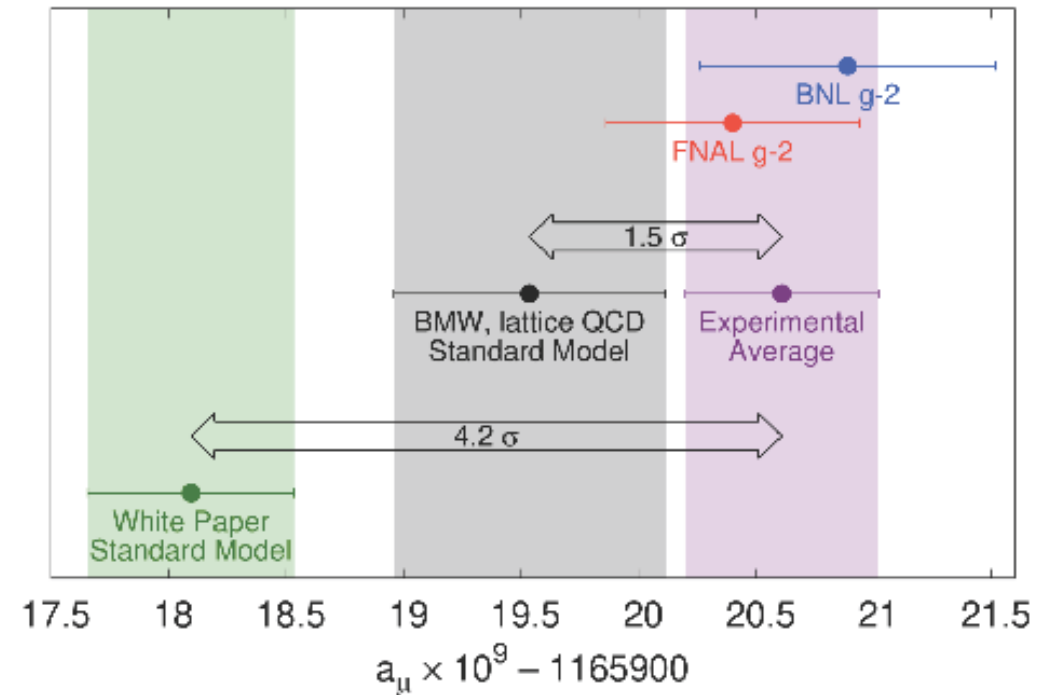
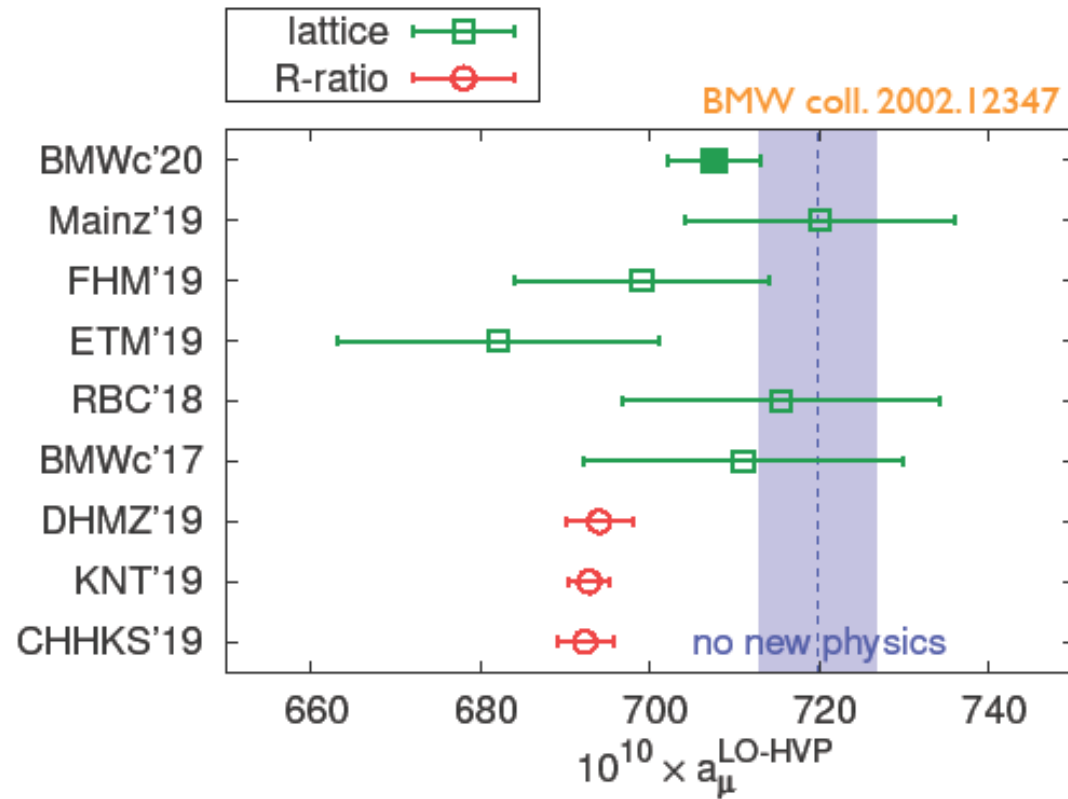
DB, MG, KM, SP, PRD107 (2023) 074001 [2211.11055 [hep-ph]]

GB, DB, MG, AK, KM, SP, PRLxxx (2023) [2306.16808 [hep-ph]]

GB, DB, MG, AK, KM, SP, arXiv: 2311.09523 [hep-ph]

CONTEXT: CURRENT FORMS OF THE LATTICE-DISPERSIVE HVP DISCREPANCY

SM expectations for a_μ with dispersive vs lattice HVP

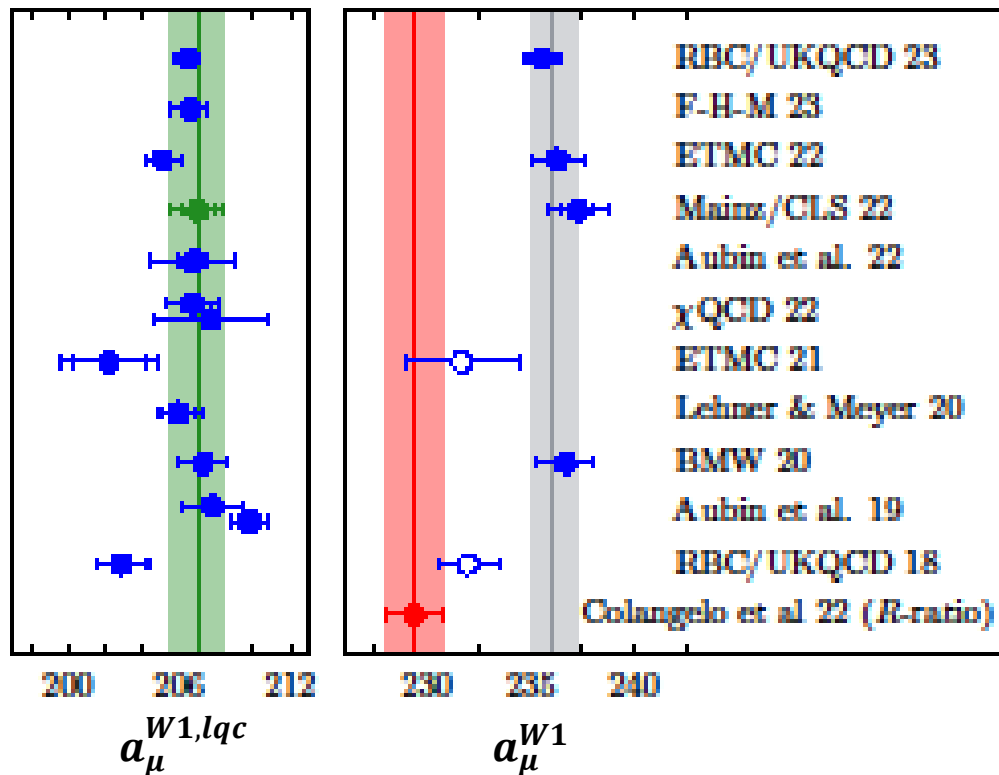


Post-FNAL Run2/3: $4.2 \sigma \rightarrow 5.0 \sigma$

CONTEXT: RBC/UKQCD intermediate window (W1) quantities ($\times 10^{10}$)

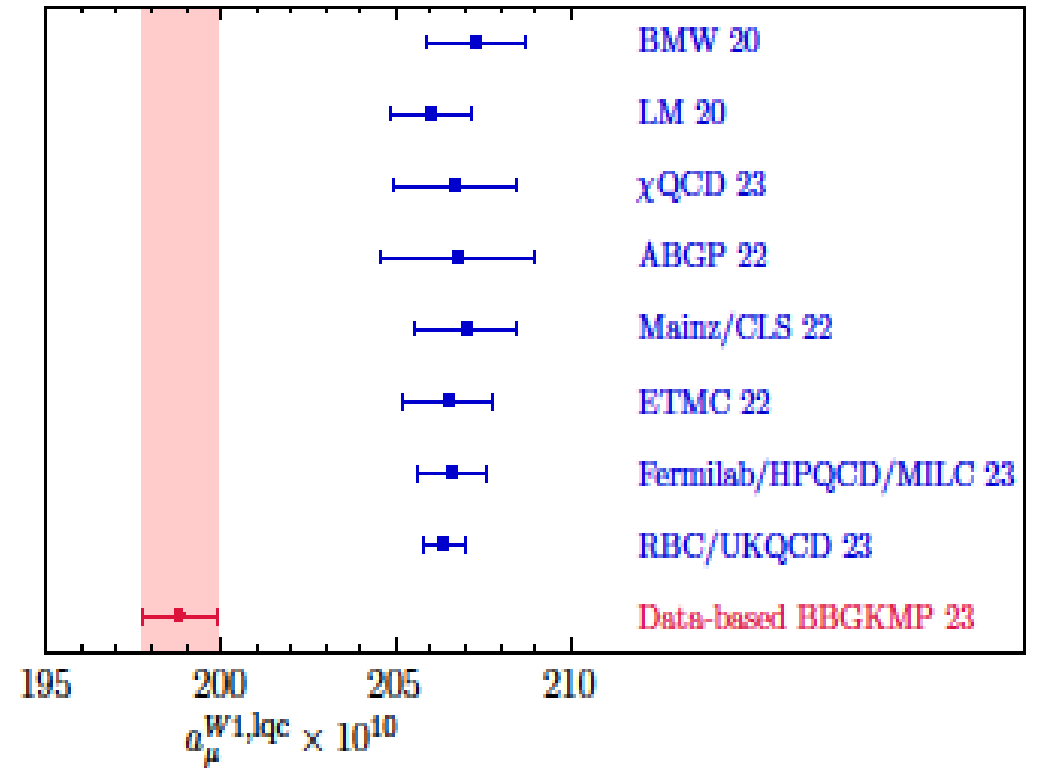
- The full intermediate window a_μ^{W1}

H. Wittig, EW Moriond 2306.04165



- IL, lqc intermediate window $a_\mu^{W1,lqc}$

GB, DB, MG, AK, KM, SP [PRLxxx [2306.16808] and below]



NOTATION, CONVENTIONS, FLAVOR DECOMPOSITIONS

$$(q_\mu q_\nu - q^2 g_{\mu\nu}) \Pi_{EM}(q^2) = i \int d^4x e^{iq \cdot x} \langle O | T (J_\mu^{EM}(x) J_\nu^{EM}(0)) | O \rangle$$

$$\hat{\Pi}_{EM}(q^2) \equiv \Pi_{EM}(q^2) - \Pi_{EM}(0) = q^2 \int_{m_\pi^2}^{\infty} ds \frac{\rho_{EM}(s)}{s(s - q^2 + i\epsilon)} \quad \rho_{EM}(s) \equiv \frac{1}{\pi} \text{Im} \Pi_{EM}(s)$$

SU(3)_F decompositions

$$\begin{aligned} J_\mu^{EM} &= V_\mu^3 + \frac{1}{\sqrt{3}} V_\mu^8 \equiv J_\mu^{EM,3} + J_\mu^{EM,8} + \dots & \hat{\Pi}_{EM}(Q^2) &= \hat{\Pi}_{EM}^{33}(Q^2) + \frac{2}{\sqrt{3}} \hat{\Pi}_{EM}^{38}(Q^2) + \frac{1}{3} \hat{\Pi}_{EM}^{88}(Q^2) \\ &= \frac{1}{2} (u\gamma_\mu u - d\gamma_\mu d) + \frac{1}{6} (u\gamma_\mu u + d\gamma_\mu d - 2s\gamma_\mu s) + \dots & &= \hat{\Pi}_{EM}^{I=1}(Q^2) + \hat{\Pi}_{EM}^{MI}(Q^2) + \hat{\Pi}_{EM}^{I=0}(Q^2) \end{aligned}$$

I=1, G-parity +

I=0, G-parity -

+ similarly for $\rho_{EM}(s)$

$$a_\mu^X = a_\mu^{X,33} + \frac{2}{\sqrt{3}} a_\mu^{X,38} + \frac{1}{3} a_\mu^{X,88} \equiv a_\mu^{X,I=1} + a_\mu^{X,MI} + a_\mu^{X,I=0}$$

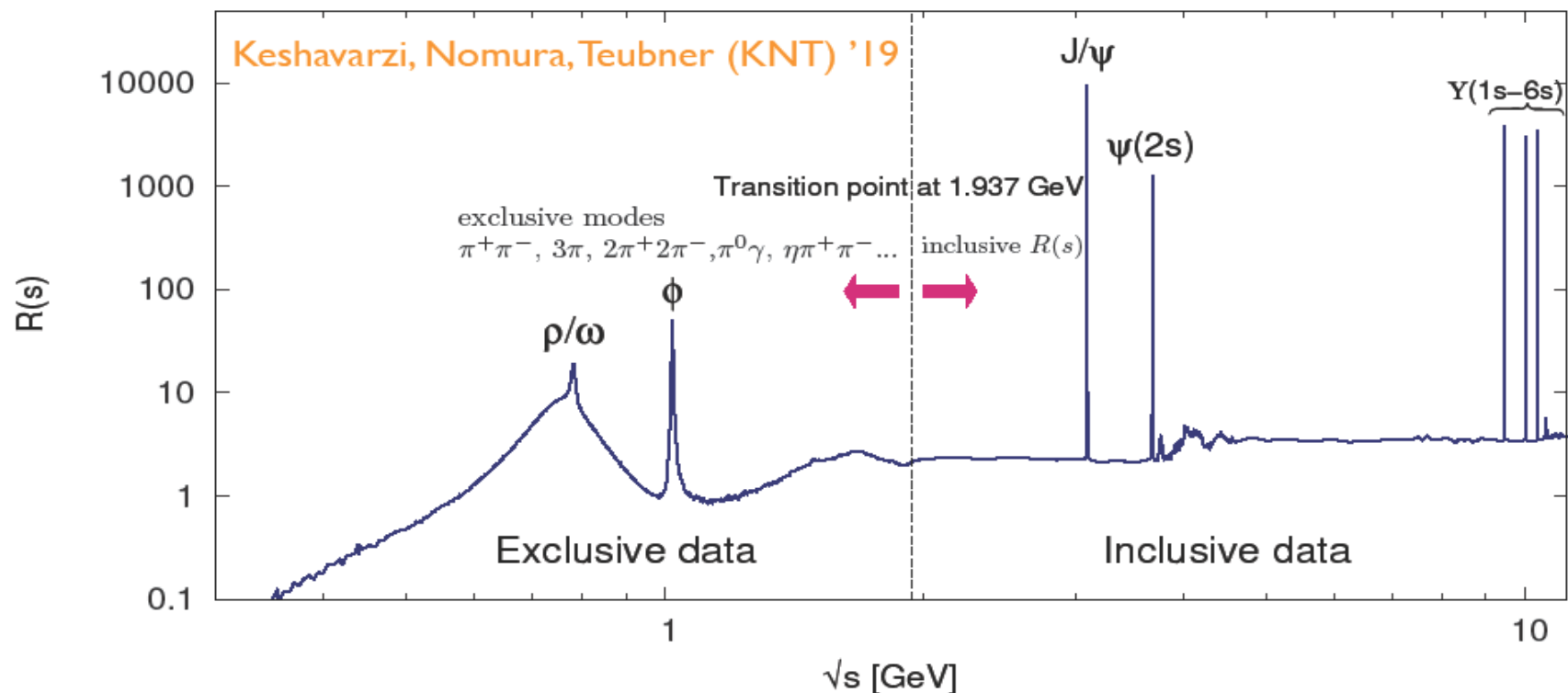
NOTATION and CONVENTIONS: a_μ^{HVP} DISPERSIVE REPRESENTATION

$$a_\mu^{\text{HVP}} = \frac{4\alpha^2 m_\mu^2}{3} \int_{m_\pi^2}^{\infty} ds \frac{\hat{K}(s)}{s^2} \rho_{\text{EM}}(s)$$

$$\rho_{\text{EM}}(s) = \frac{1}{12\pi^2} R(s)$$

Compilation of R -ratio data

(see also Davier et al '19, Jegerlehner '16)



NOTATION and CONVENTIONS: a_μ LATTICE REPRESENTATION

$$C(t) = \frac{1}{3} \sum_{i=1}^3 \int d^3x \langle j_i^{\text{EM}}(\vec{x}, t) j_i^{\text{EM}}(0) \rangle = \frac{1}{2} \int_{m_\pi^2}^{\infty} ds \sqrt{s} e^{-\sqrt{s}t} \rho_{\text{EM}}(s) \quad (t > 0)$$

Bernecker and Meyer '11

$$\hat{\Pi}(Q^2) = \int_0^\infty dt \left(\frac{4 \sin^2(Qt/2)}{Q^2} - t^2 \right) C(t)$$

Leading order contribution to a_μ^{HVP}

$$a_\mu^{\text{HVP}} = 2 \int_0^\infty dt w(t) C(t)$$

$$\frac{\hat{K}(s)}{s^2} = \frac{3\sqrt{s}}{4\alpha^2 m_\mu^2} \int_0^\infty dt w(t) e^{-\sqrt{s}t}$$

Light flavor lattice contributions

- isospin limit (IL) light-quark (u, d) connected (lqc): **I=0 and 1**
- IL strange-quark connected (sconn) and uds disconnected (disc): **I=0 only**
- EM (connected and disconnected): **all of I=0, I=1 and MI**
- strong isospin-breaking (SIB) (connected and disconnected): **to $O(m_d - m_u)$: MI only**

ISOSPIN LIMIT RELATIONS

$$\rho_{EM}^{IL,lqc} = \frac{10}{9} \rho_{EM}^{I-1}$$

$$\rho_{EM}^{sconn+disc} = \rho_{EM}^{I-0} - \frac{1}{9} \rho_{EM}^{I-1}$$

$$\hat{\Pi}_{EM}^{IL,lqc} = \frac{10}{9} \hat{\Pi}_{EM}^{I-1}$$

$$\hat{\Pi}_{EM}^{sconn+disc} = \hat{\Pi}_{EM}^{I-0} - \frac{1}{9} \hat{\Pi}_{EM}^{I-1}$$

$$\alpha_{\mu}^{IL,lqc} = \frac{10}{9} \alpha_{\mu}^{I-1}$$

$$\alpha_{\mu}^{sconn+disc} = \alpha_{\mu}^{I-0} - \frac{1}{9} \alpha_{\mu}^{I-1}$$

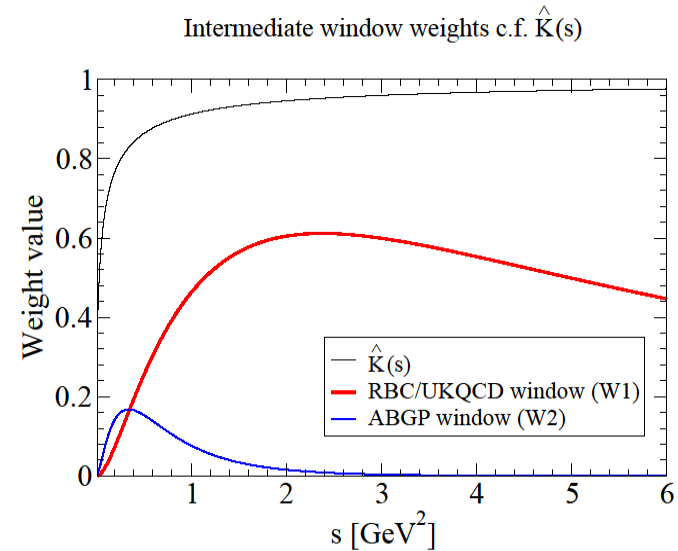
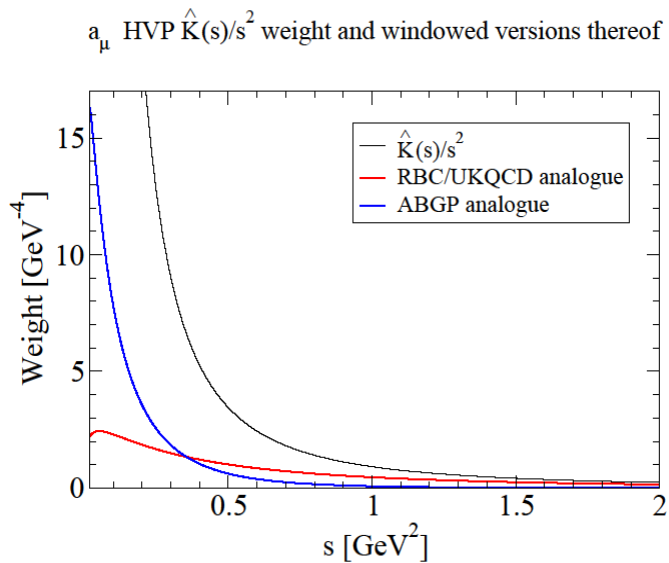
with similar representations for re-weighted (windowed) IL, lqc and sconn+disc integrals

LATTICE-MOTIVATED INTERMEDIATE WINDOW QUANTITIES

- Reduce lattice errors by cutting out short- and long-t contributions
- RBC/UKQCD style intermediate-window reweighting:

$$a_\mu^W = 2 \int_0^\infty dt f_W(t; t_0, t_1, \Delta) [w(t)C(t)] \quad f_W(t; t_0, t_1, \Delta) = \frac{1}{2} \left[\tanh\left(\frac{t-t_0}{\Delta}\right) - \tanh\left(\frac{t-t_1}{\Delta}\right) \right]$$

- RBC/UKQCD (W1): $t_0 = 0.4$ fm, $t_1 = 1.0$ fm, $\Delta = 0.15$ fm
- ABGP (W2): $t_0 = 1.5$ fm, $t_1 = 1.9$ fm, $\Delta = 0.15$ fm



“WINDOWS” EMPHASIZING DIFFERENT REGIONS IN s

- **Examples of motivation for focusing on specific regions in s :**
 - BaBar/KLOE/CMD-3 $\pi\pi$ data discrepancies in dominant ρ peak region
 - EM/ τ +CVC discrepancies for 4π contributions at higher s
- **Key question: can this be done without blowing up errors on the corresponding lattice quantities? Answer: Yes: exponential-weight sum rules**
 - Appropriately chosen/tuned linear combinations of exponentials in Euclidean t
 - Tuning to focus of desired region of s
 - $\{t_k\}$ chosen to avoid large Euclidean t and control lattice errors

EXPONENTIAL WEIGHT SUM RULES (EWSRs)

$$\text{For } w_n(E) = \sum_{j=1}^n x_j E^2 e^{-Et_j}, \quad C(t) = \int_{E_{th}}^{\infty} dE E^2 e^{-Et} \rho(E^2), \quad t > 0$$

Exponential-weight sum rules

$$\Rightarrow \int_{E_{th}}^{\infty} dE w_n(E) \rho(E) = \sum_{j=1}^n x_j C(t_j)$$

R(s) data

lattice

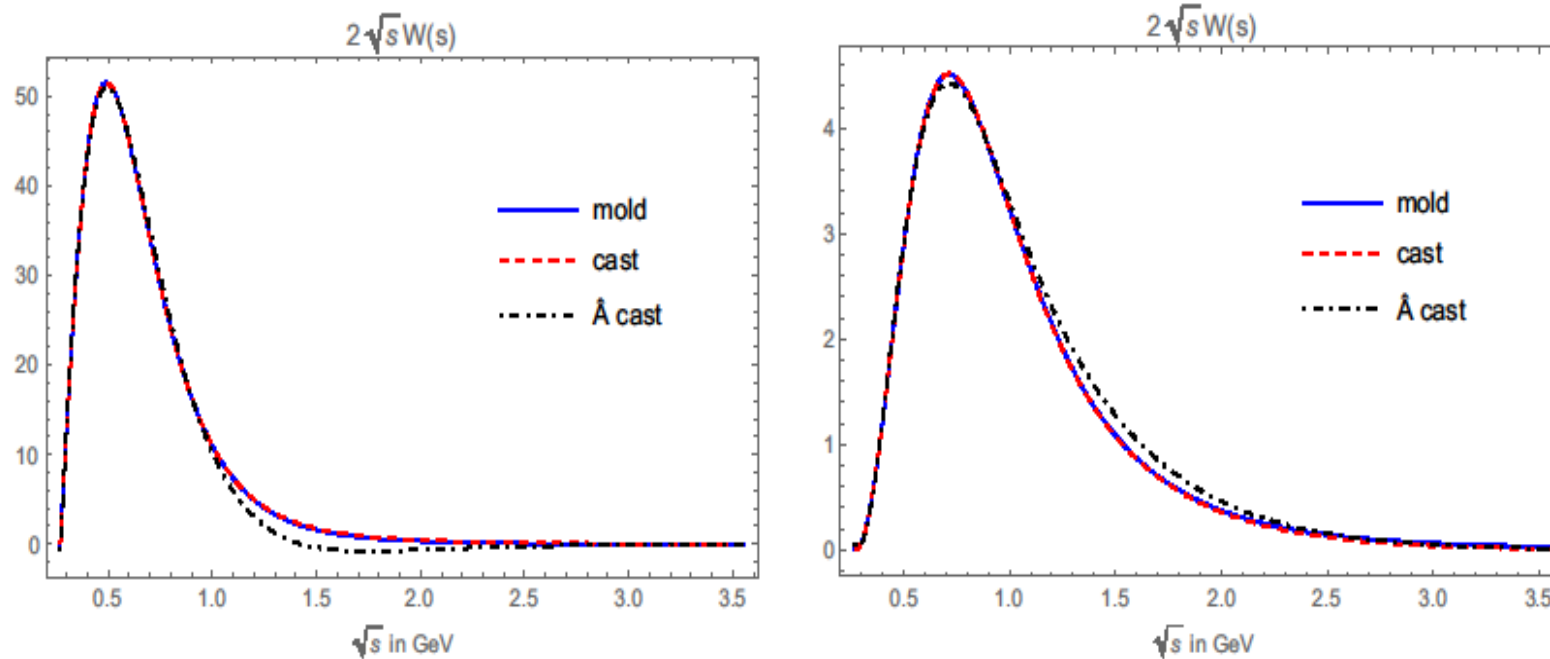
Hansen, Lupo, Tantalo 2019

Hashimoto, Ishikawa 2020

Basic analysis strategy [Boito, Golterman, KM, Peris, 2022]

- Pick a physically interesting $w(s)=2E W(E)$ (**the “mold”**)
- Build an approximation, $w_n(E; \{x_j\}, \{t_j\})$ (**the “cast”**) using a small number of externally chosen $\{t_j\}$ and appropriately adjusted $\{x_j\}$
- Choose $\{t_j\}$ to keep all $C(t_j)$ errors small (avoiding large t by construction)
- **Provided the localization-in- s of the “cast” is similar to that of the “mold”, throw away the mold and work instead with the exact cast sum rule**

“IMPROVED” VS “UNIMPROVED” EWSR CASTS



- “Unimproved” casts from strict HLT implementation; “improved” from reduced fit condition number construction
- “Improved” casts (slightly) less similar to the “molds”
- However, still rather close to those “molds”; hence provide essentially the same localization-in-s as the original “molds” or unimproved “casts”

RESULTS OF THE IMPROVED EWSR “CAST” CONSTRUCTION

		<i>R(s) data</i>		<i>rational weight</i>	W'	<i>exponential weight</i>
	R-ratio	rel. error	lattice	rel. error	lattice	rel. error
W_{15}	0.4756(16)	0.3%	0.468(26)	5.6%	0.496(17)	3.4%
W_{25}	0.08912(34)	0.4%	0.0838(33)	3.9%	0.0798(18)	2.3%

Lattice errors: ABGP22 IL, lqc only
avoid comparing central values

improved exponential weights

	lattice	rel. error
\widehat{W}_{15}	0.4669(68)	1.5%
\widehat{W}_{25}	0.0824(10)	1.2%

DB, Golterman, Maltman, and Peris, '22

- Significant reduction in lattice errors (though still ~ 3 -5 larger than dispersive)
- Further improvement possible (e.g., through modified $\{t_j\}$ set/range choices) but best explored in conjunction with detailed error studies with new lattice data
- Further reduction in lattice errors also expected c.f. ABGP22

PART II: IL, lqc AND sconn+disc RESULTS

- **Data input for the dispersive side of IL, lqc and sconn+disc sum rules**
 - Need s-dependent exclusive-mode input: here, from KNT19 (to $E_{\text{CM}}=1.937$ GeV)
 - G-parity $l=0, 1$ separation for G-parity eigenstate exclusive modes
 - External input for dominant G-parity-ambiguous modes ($l=1$ $K\bar{K}$ from **BaBar 2018** $\tau \rightarrow K\bar{K} \nu_\tau + \text{CVC}$, **BaBar 2007** Dalitz plot $l=0/1$ separation for $K\bar{K}\pi$, **PDG** ρ, ω, ϕ EM decay constants and $\pi^0\gamma, \eta\gamma$ widths for $\pi^0\gamma, \eta\gamma$ $l=0/1/MI$ separation)
 - Maximally conservative anti-correlated $50 \pm 50\%$ split if no external input
 - pQCD(+DVs) for inclusive contributions ($E_{\text{CM}} > 1.937$ GeV)
 - Small inclusive $l=0, 1$ EM IB corrections from lattice
 - Data-based corrections for MI EM+SIB contamination of nominally $l=0, 1$ sums
 - ❖ dominant ρ - ω region $2\pi, 3\pi$: **Hoferichter et al. 2022/23** (dispersive)
 - ❖ other nominally $l=0, 1$ modes: $O(1\%)$ additional uncertainty estimate
- **Here: new IL, lqc and sconn+disc results, including windows**

ANATOMY OF THE DATA-BASED DETERMINATION OF $a_\mu^{HVP,lqc} = a_\mu^{lqc,IL}$

- With KNT19 input:

$$a_\mu^{lqc,IL} = \left(\frac{10}{9} \right) \left(\underset{\substack{\text{G-par +} \\ 95\%}}{543.2(2.1)} + \underset{\substack{\text{G-par ambig} \\ 0.56\%}}{3.2(1.0)} + \underset{\substack{pQCD \\ 5.0\%}}{28.27(2)} + \underset{\substack{DVs}}{0.26(12)} \right) + \underset{\substack{EM IB \\ 0.15\%}}{0.93(59)} - \underset{\substack{MI IB \\ -0.66\%}}{4.21(47)}$$

Colangelo, Hoferichter, Kubis, Stoffer 2022 (CHKS22)

- Full $a_\mu^{lqc,IL} \times 10^{10}$ results:

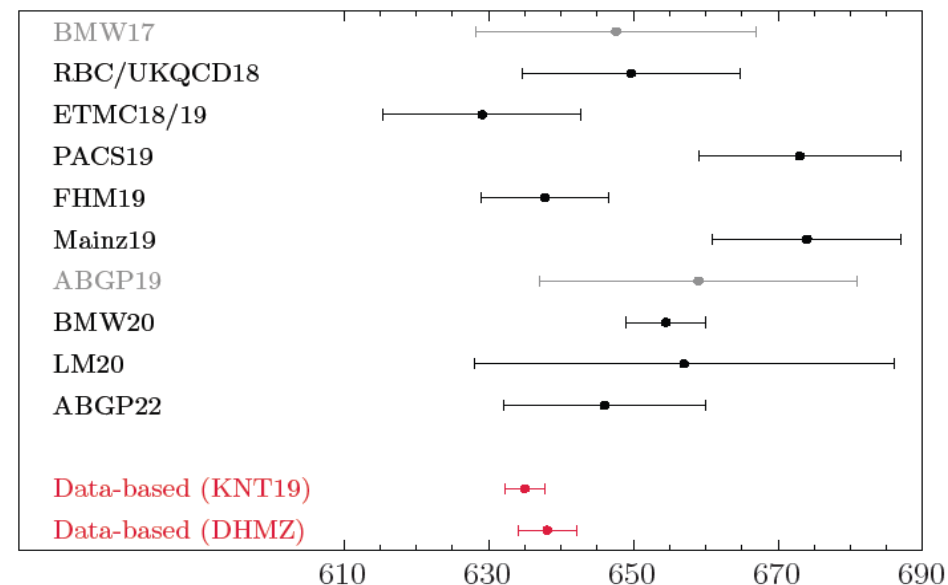
$$a_\mu^{lqc,IL} = 635.2(2.7) \quad (\text{KNT})$$

$$a_\mu^{lqc,IL} = 638.3(4.1) \quad (\text{DHMZ})$$

- Some tension with lattice (BMW)

light-quark connected

(88% of this result comes from pi+pi)



RBC/UKQCD INTERMEDIATE WINDOW IL,l_qc RESULTS

G=+ mode X	$a_{\mu,X}^{W1} \times 10^{10}$
low-s $\pi^+ \pi^-$	0.02(00)
$\pi^+ \pi^-$	144.13(49)
$2\pi^+ 2\pi^-$	9.29(13)
$\pi^+ \pi^- 2\pi^0$	11.94(48)
$3\pi^+ 3\pi^-$ (no ω)	0.14(01)
$2\pi^+ 2\pi^- 2\pi^0$ (no η)	0.83(11)
$\pi^+ \pi^- 4\pi^0$ (no η)	0.13(13)
$\eta\pi^+ \pi^-$	0.85(03)
$\eta 2\pi^+ 2\pi^-$	0.05(01)
$\eta\pi^+ \pi^- 2\pi^0$	0.07(01)
$\omega(\rightarrow \pi^0 \gamma)\pi^0$	0.53(01)
$\omega(\rightarrow npp)3\pi$	0.10(02)
$\omega\eta\pi^0$	0.15(03)
TOTAL	168.24(72)

$a_{\mu}^{W1,lqc}$ contributions (in units of 10^{10})

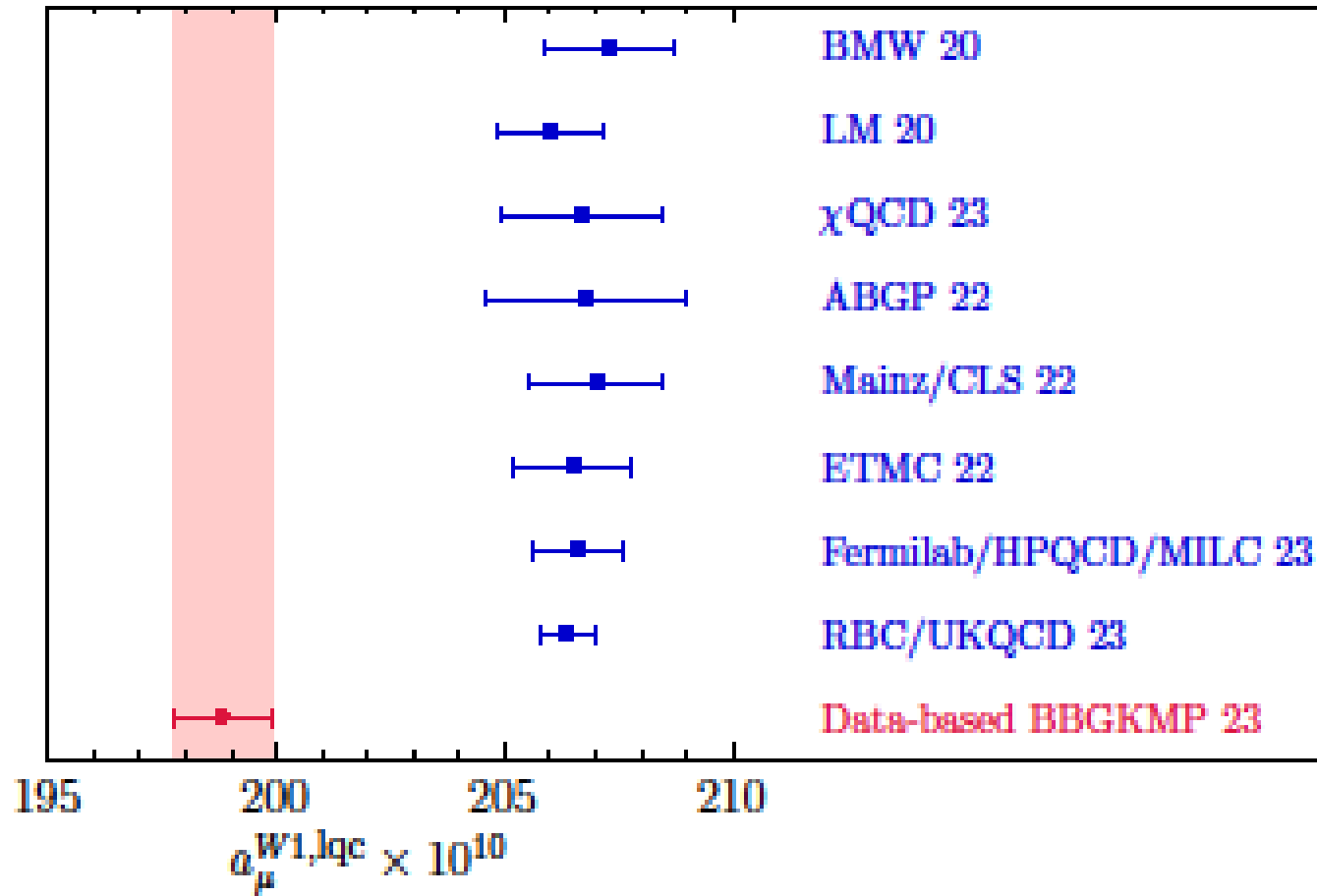
- G=+: 186.93(80)
- $K\bar{K}$: 0.58(7)
- $K\bar{K}\pi$: 0.52(9)
- $K\bar{K}\pi\pi$: 0.60(60)
- $\pi^0\gamma+\eta\gamma$: 0.14(1)
- other mixed G: 0.05(5)
- pQCD $\pm DV$ s: 10.90 ± 0.17
- EM corr'n: -0.04(6)
- 2π (\pm other) MI corr'n: $-0.96(7) \pm 0.29$

[CHKS22 2π MI corr'n: JHEP 10 (2022) 032]

$$a_{\mu}^{W1,lqc} = 198.9(1.1) \times 10^{-10}$$

G. Benton, DB, MG, AK, KM, SP [PRLxxx, 2306.16808]

RBC/UKQCD INTERMEDIATE WINDOW DISPERSIVE IL, I_{qc} c.f. LATTICE



- Very significant tension between dispersive and lattice W1 IL, I_{qc} results

IL, I_{qc} DISPERSIVE vs LATTICE RESULTS FOR OTHER INTERMEDIATE WINDOWS

- Lattice EM results not available so neglect EM $I=0, 1$ corrections for now (plausible based on RBC/UKQCD intermediate window result)
- For IL, I_{qc} case, windowed versions of CHKS22 2π MI correction (provided by M. Hoferichter and P. Stoffer: thanks!)
- For sconn+disc case, windowed ρ - ω region 3π MI correction of Hoferichter, Hoid, Kubis, Schuh (JHEP 08 (2023) 208) (HHKS23)
- **Compare IL, I_{qc} dispersive and ABGP22-based lattice results**

ABGP22 INTERMEDIATE WINDOW (W2) RESULTS

- RBC/UKQCD-style intermediate window, designed to be longer distance, more amenable to possible use of ChPT

lattice results

Light-quark connected from **KNT19** R(s) data

$$a_{\mu}^{W2,lqc} = 93.75(36) \times 10^{-10}$$

Aubin, Blum, Golterman, Peris '22

$$a_{\mu}^{W2,lqc} = 102.1(2.4) \times 10^{-10}$$

Fermilab/HPQCD/MILC '23

$$a_{\mu}^{W2,lqc} = 100.7(3.2) \times 10^{-10}$$

- Once more, dispersive-lattice tension, but reduction in lattice errors needed to sharpen the dispersive-lattice comparison

IMPROVED EWSR WEIGHT (\widehat{W}_{15} , \widehat{W}_{25}) IL, lqc RESULTS

- $I_W^{lqc} \equiv \int_{th}^{\infty} ds W(s) \rho_{EM}^{IL,lqc}(s)$

Dispersive

$$I_{\widehat{W}_{15}}^{IL,lqc} = 42.80(16) \times 10^{-2}$$

\longleftrightarrow
5.6 σ

ABGP Lattice

$$I_{\widehat{W}_{15}}^{IL,lqc} = 46.69(68) \times 10^{-2}$$

$$I_{\widehat{W}_{25}}^{IL,lqc} = 78.99(45) \times 10^{-3}$$

\longleftrightarrow
3.1 σ

$$I_{\widehat{W}_{25}}^{IL,lqc} = 82.4(1.0) \times 10^{-3}$$

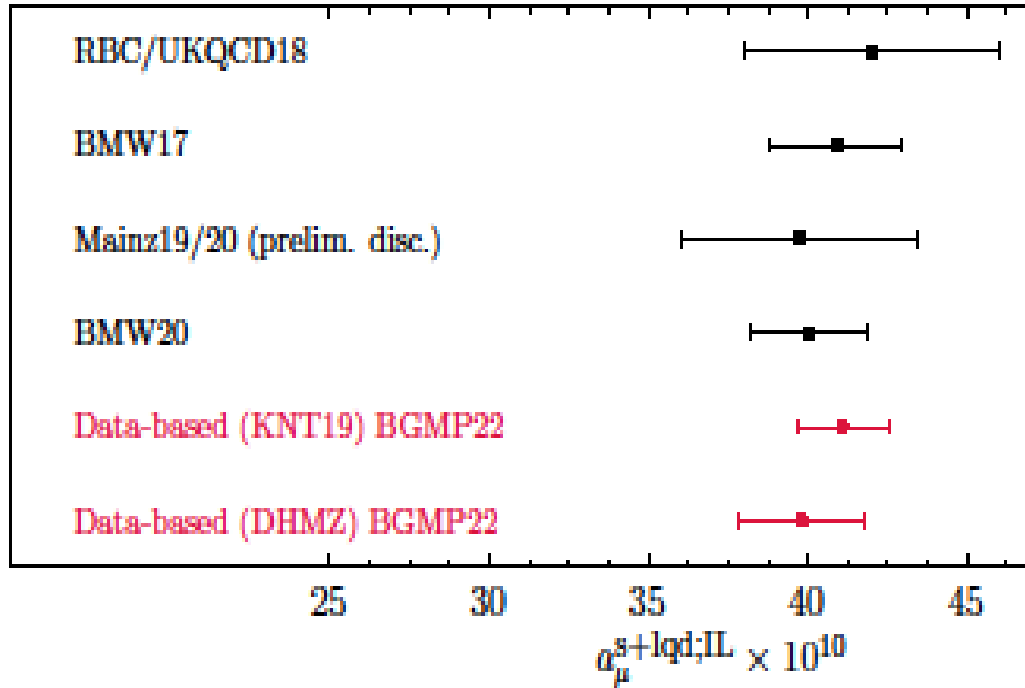
Benton, Boito, Golterman, Keshavarzi,
Maltman, Peris, 2311.09523

systematic errors on lattice
results still to be assessed

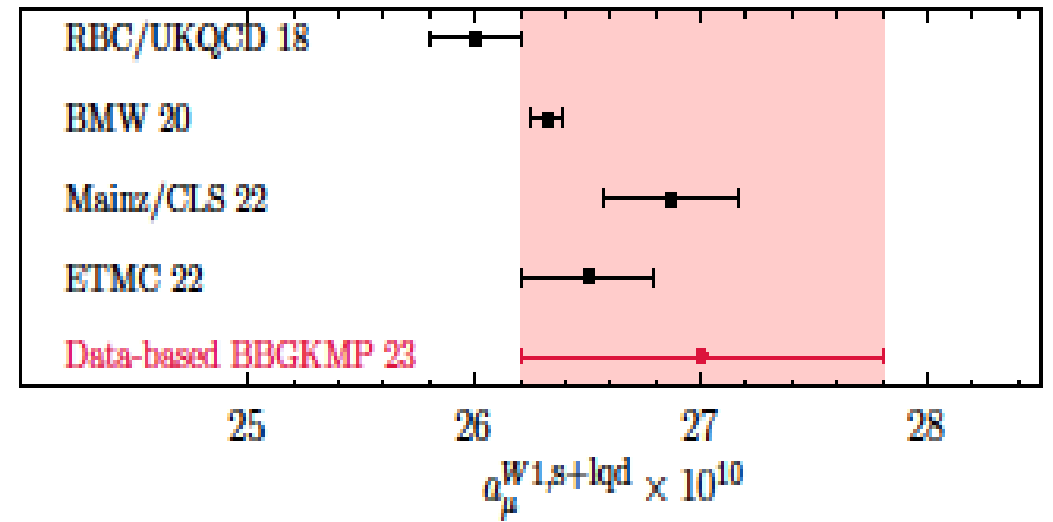
- Another sign of tension between dispersive and lattice IL, lqc results

sconn+disc $a_\mu^{sconn+disc} = a_\mu^{s+lqd,IL}$, $a_\mu^{W1,s+lqd}$ results

- Update of PRD105 (2022) 093003 $a_\mu^{s+lqd,IL}$



- RBC/UKQCD window version $a_\mu^{W1,s+lqd}$



POTENTIAL IMPACT OF THE NEW CMD-3 $\pi\pi$ DATA

- **Interim conclusion:** current published cross sections lead to
 - good lattice/data-driven agreement for sconn+disc quantities
 - significant disagreement (data-driven<lattice) for lqc quantities
 - **⇒ lattice vs. data-driven discrepancy essentially all from lqc contribution**
- **However, new CMD-3 study [2302.8834 [hep-ex]] finds ρ peak region $\pi\pi$ cross sections significantly higher than CMD-2, BaBar, KLOE, BESIII, SND**
 - Still undergoing scrutiny, but no obvious problems to date
 - Replacing $\pi\pi$ HVP in CMD-3 region with CMD-3 only reduces SM-expt'l a_μ discrepancy to 0.9σ [CMD-3 2309.12910 [hep-ex] and many others]
 - **What about the impact on the KNT19-based lqc discrepancies above?**

CAUTION: PRELIMINARY EXPLORATION ONLY

i.e., NOT a new KNT-style 2023 2π combination

A. Keshavarzi Lattice 2023: Impact on $a_\mu^{W1,lqc}$ and a_μ^{HVP}

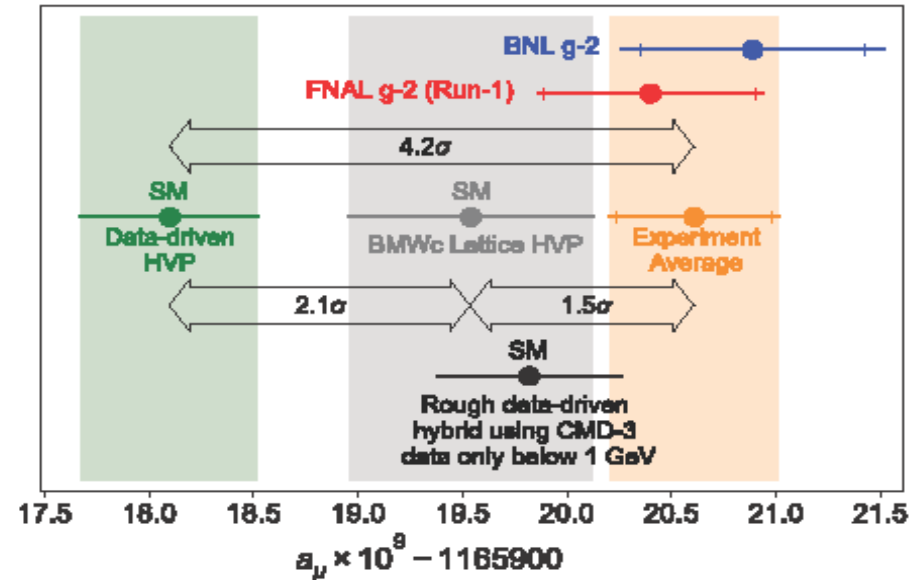
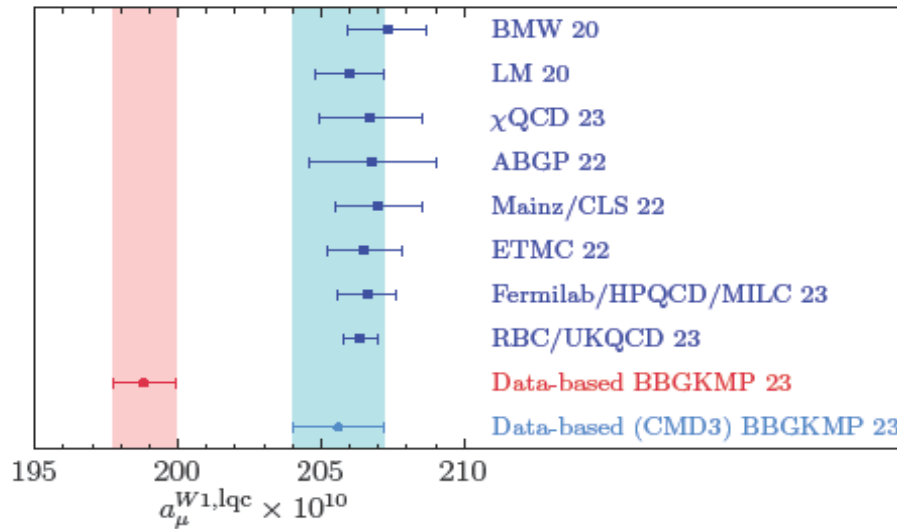


Impact of CMD-3

CMD-3 [F. Ignatov et al, arXiv:2302.08834]

DISCLAIMER: these are **NOT** new updates or combinations including the CMD-3 data – simply demonstrations of the impact of the CMD-3 data alone.

In collaboration with Genessa Benton, Diogo Boito, Maarten Golterman, Kim Maltman & Santi Peris [arXiv:2306.16808].



IMPORTANT: THIS PLOT IS VERY ROUGH!

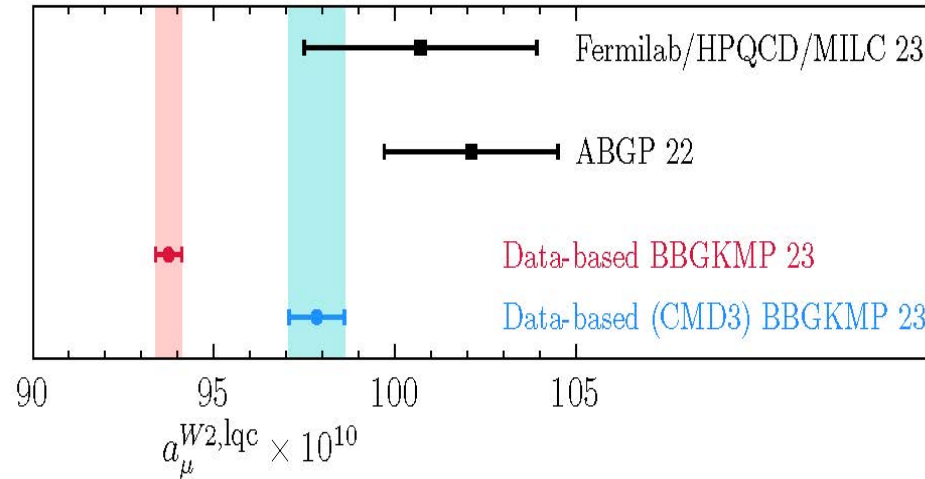
- TI White Paper result has been substituted by CMD-3 only for 0.33 → 1.0 GeV.
- The NLO HVP has not been updated.
- It is purely for demonstration purposes → should not be taken as final!

Until differences are understood, and intense scrutiny of new/old results is complete, no conclusions can be drawn about the validity of SM estimates. A lot of work still to be done...

With CMD-3: $205.6(1.6) \times 10^{-10}$

Impact on the IL, lqc \widehat{W}_2 , \widehat{W}_{15} and \widehat{W}_{25} results

- KNT19 $a_\mu^{W2,lqc}$



- KNT19 $I_{\widehat{W}_{15}}^{IL,lqc}$: $0.4280(16) \rightarrow 0.4483(37)$ c.f. lattice $0.4669(58)$ ($5.6 \sigma \rightarrow 2.7 \sigma$)
- KNT19 $I_{\widehat{W}_{25}}^{IL,lqc}$: $0.0790(5) \rightarrow 0.0815(6)$ c.f. lattice $0.0824(10)$ ($3.1 \sigma \rightarrow 0.8 \sigma$)
- **All dispersive-lattice differences strongly reduced with CMD-3 $\pi\pi$ input**

CONCLUSIONS

- With current EM $R(s)$ data, significant data-driven/lattice discrepancies, especially for IL, lqc RBC/UKQCD intermediate window (W1) and improved EWSR (\widehat{W}_{15} , \widehat{W}_{25}) weightings
- Currently known lattice/data-driven discrepancies all disappear if CMD-3 $\pi\pi$ cross-section results correct [resolution of CMD-3/BaBar/KLOE discrepancy of high interest]
- (Improved) EWSRs as a potential approach for exploring potential discrepancies in different regions of s (in this talk, focusing on the ρ peak region, but alternatives focusing on other regions of interest as well)
- $C(t)$ results needed to determine a_μ^{HVP} and a_μ^{W1} and/or components thereof also provide results for the lattice side of any related EWSR: further exploration of EWSR weight choices in conjunction with new lattice data thus also of interest

BACKUP SLIDES

HLT IMPLEMENTATION OF THE EWSR “CAST” CONSTRUCTION

Given the mold function, minimize $\int_{E_{\text{th}}}^{\infty} dE |w_n(E; \{t_j\}, \{x_j\})/E^2 - 2W(E^2)/E|^2$

which has the solution

$$x_i = \sum_{j=1}^n A_{ij}^{-1} f_j$$

with

$$A_{ij} = \int_{E_{\text{th}}}^{\infty} dE e^{-(t_i+t_j)E},$$

$$f_i = 2 \int_{E_{\text{th}}}^{\infty} dE e^{-t_i E} W(E^2)/E$$

Hansen, Lupo, Tantaló '19

For a chosen set of time values this gives the coefficients x_j

HLT IMPLEMENTATION OF THE EWSR “CAST” CONSTRUCTION

Given the mold function, minimize $\int_{E_{\text{th}}}^{\infty} dE |w_n(E; \{t_j\}, \{x_j\})/E^2 - 2W(E^2)/E|^2$

which has the solution

$$x_i = \sum_{j=1}^n A_{ij}^{-1} f_j$$

with

$$A_{ij} = \int_{E_{\text{th}}}^{\infty} dE e^{-(t_i+t_j)E},$$

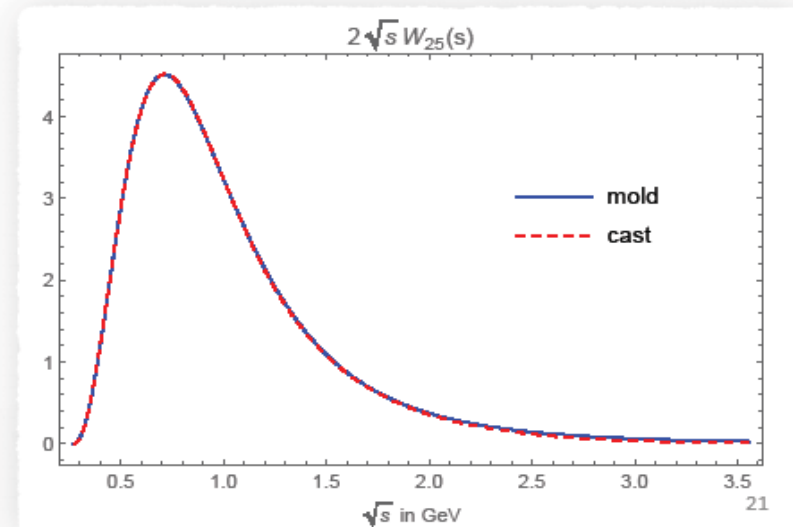
$$f_i = 2 \int_{E_{\text{th}}}^{\infty} dE e^{-t_i E} W(E^2)/E$$

Hansen, Lupo, Tantaló '19

For a chosen set of time values this gives the coefficients x_j

$$t_j = 3, 6, 9, 12, 15 \text{ GeV}^{-1} \approx 0.6, 1.2, 1.8, 2.4, 3 \text{ fm}$$

$$W'_{2,5}: x_1 = 34.0249, \quad x_2 = 870.640, \quad x_3 = -5501.14, \\ x_4 = 9933.01, \quad x_5 = -5284.24.$$



HLT IMPLEMENTATION OF THE EWSR “CAST” CONSTRUCTION

Given the mold function, minimize $\int_{E_{th}}^{\infty} dE |w_n(E; \{t_j\}, \{x_j\})/E^2 - 2W(E^2)/E|^2$

which has the solution

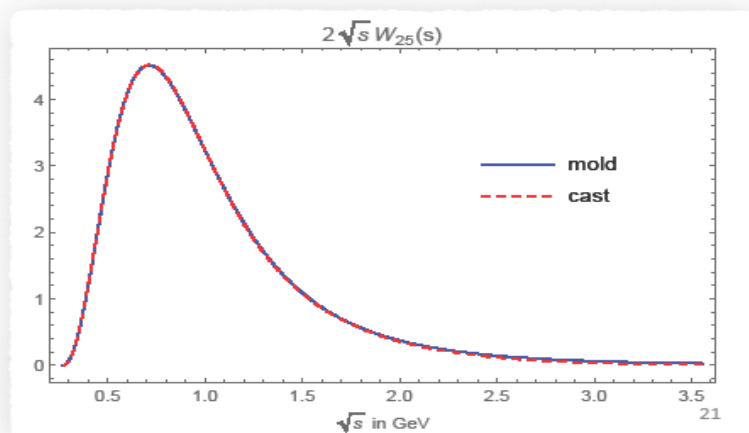
$$x_i = \sum_{j=1}^n A_{ij}^{-1} f_j \quad \text{with} \quad A_{ij} = \int_{E_{th}}^{\infty} dE e^{-(t_i+t_j)E}, \quad f_i = 2 \int_{E_{th}}^{\infty} dE e^{-t_i E} W(E^2)/E$$

Hansen, Lupo, Tantaló '19

For a chosen set of time values this gives the coefficients x_j

$$t_j = 3, 6, 9, 12, 15 \text{ GeV}^{-1} \approx 0.6, 1.2, 1.8, 2.4, 3 \text{ fm}$$

$$W'_{2,5}: x_1 = 34.0249, \quad x_2 = 870.640, \quad x_3 = -5501.14, \\ x_4 = 9933.01, \quad x_5 = -5284.24.$$



	R(s) data		rational weight		exponential weight	
	R-ratio	rel. error	lattice	rel. error	lattice	rel. error
W_{15}	0.4756(16)	0.3%	0.468(26)	5.6%	0.496(17)	3.4%
W_{25}	0.08912(34)	0.4%	0.0838(33)	3.9%	0.0798(18)	2.3%

Lattice errors: ABGP22 IL, lqc only
avoid comparing central values

AN IMPROVED EWSR “CAST” CONSTRUCTION

- The HLT minimization of $\int_{E_{\text{th}}}^{\infty} dE |w_n(E; \{t_j\}, \{x_j\})/E^2 - 2W(E^2)/E|^2$

$$x_i = \sum_{j=1}^n A_{ij}^{-1} f_j$$

with

$$A_{ij} = \int_{E_{\text{th}}}^{\infty} dE e^{-(t_i+t_j)E},$$

$$f_i = 2 \int_{E_{\text{th}}}^{\infty} dE e^{-t_i E} W(E^2)/E$$

can be modified to remove the small eigenvalues of the matrix A via

$$\hat{A}(\lambda) = (1 - \lambda)A + \lambda \mathbf{1}_n$$

This removes eigenvalues $< \lambda$ and reduce the range of the values of $\{x_i\}$.

$$\lambda = 10^{-9}$$

$$\hat{W}_{2,5}: x_1 = 44.8916, \quad x_2 = 590.933, \quad x_3 = -3373.53,$$

$$x_4 = 3716.86, \quad x_5 = 879.149.$$

significantly reduced values
of x_4 and x_5

$$W'_{2,5}: x_1 = 34.0249, \quad x_2 = 870.640, \quad x_3 = -5501.14,$$

$$x_4 = 9933.01, \quad x_5 = -5284.24.$$

CMD-3 vs THE KNT19 COMBINATION (from A. Keshavarzi, Lattice 2023)



The University of Manchester

CMD-3 compared to KNT19

In collaboration with Genessa Benton, Diogo Boito, Maarten Golterman, Kim Maltman & Santi Peris.

CMD-3 [F. Ignatov et al, arXiv:2302.08834]

To be able to compare CMD-3 with KNT19 data combination:

- Data published as pion form factor, $|F_\pi|^2$.
- Must subtract vacuum polarisation effects using Fedor Ignatov's VP correction update.
- Must include final-state-radiation effects.
- Put data on fine, common binning.

In the full 2π data combination range, the KNT19 analysis found:

$$a_\mu^{\pi^+\pi^-}(0.305 \rightarrow 1.937 \text{ GeV}) = (503.46 \pm 1.91) \times 10^{-10}.$$

Replacing KNT19 2π data in the region $0.33 \rightarrow 1.20 \text{ GeV}$ with CMD-3 data:

$$a_\mu^{\pi^+\pi^-}(0.305 \rightarrow 1.937 \text{ GeV}) = (525.17 \pm 4.18) \times 10^{-10}.$$

Neglecting possible correlations between e.g. CMD-3 and CMD-2, this results in a difference of:

$$\Delta a_\mu^{\pi^+\pi^-} = (21.71 \pm 4.96) \times 10^{-10} \rightarrow 4.4\sigma,$$

This removes the experiment vs. SM Muon g-2 discrepancy.

